The effect of oxide aperture diameter on the electrical characteristics of the GaN-based vertical cavity surface emitting laser

Azita Zandi Goharrizi[a]**, Zainuriah Hassan, and Haslan Abu Hassan**

Nano-Optoelectronics Research and Technology Laboratory, School of Physics, Universiti Sains Malaysia, 11800 Penang, Malaysia

a) *azita.zd07@student.usm.my*

Abstract: In this paper, a numerically investigation of the aperture diameter in intracavity-contacted oxide-confined GaN-based VCSEL is presented. Simulation results show that with increasing of the current aperture diameter, there is a reduction in the differential resistance of the VCSEL. The influence of oxide aperture on the threshold current has also been investigated. There is an enhancement in the threshold current of the VCSEL by increasing the oxide aperture diameter.

Keywords: laser diodes, vertical cavity surface emitting lasers, threshold current, distributed Bragg reflectors

Classification: Optoelectronics, Lasers and quantum electronics, Ultrafast optics, Silicon photonics, Planar lightwave circuits

References

[1] K. Iga, "Surface-emitting laser—Its birth and generation of new optoelectronics field," *IEEE J. Sel. Topics Quantum Electron.*, vol. 6, no. 6, pp. 1201–1215, Nov./Dec. 2000.

[2] W. W. Chow, K. D. Choquette, M. H. Crawford, K. L. Lear, and G. R. Hadley, "Design, fabrication, and performance of infrared and visible vertical-cavity surface-emitting lasers," *IEEE J. Quantum Electron.*, vol. 33, no. 10, pp. 1810–1824, Oct. 1997.

[3] E. Towe, R. F. Leheny, and A. Yang, "A historical perspective of the development of the vertical-cavity surface-emitting laser," *IEEE J. Sel. Topics Quantum Electron.*, vol. 6, no. 6, pp. 1458–1464, Nov./Dec. 2000.

[4] T. Someya, R. Werner, A. Forchel, M. Catalano, R. Cingolani, and Y. Arakawa, "Room Temperature Lasing at Blue Wavelengths in Gallium Nitride Microcavities," *Science*, vol. 285, pp. 1905–1906, Sept. 1999.

[5] R. Butté, E. Feltin, J. Dorsaz, G. Christmann, J.-F. Carlin, N. Grandjean, and M. Ilegems, "Recent Progress in the Growth of Highly Reflective Nitride-Based Distributed Bragg Reflectors and Their Use in Microcavities," *Jpn. J. Appl. Phys., Part 1*, vol. 44, no. 10, pp. 7207–7216, Oct. 2005.

[6] G. S. Huang, T. C. Lu, H. H. Yao, H. C. Kuo, and S. C. Wang, "Crack-

free GaN/AlN distributed Bragg reflectors incorporated with GaN/AlN superlattices grown by metalorganic chemical vapor deposition," *Appl. Phys. Lett.*, vol. 88, 061904, Feb. 2006.

[7] M. Arita, M. Nishioka, and Y. Arakawa, "InGaN Vertical Microcavity LEDs with a Si-Doped AlGaN/GaN Distributed Bragg Reflector," *Phys. Status Solidi A*, vol. 194, pp. 403–406, Oct. 2002.

[8] T. Ive, O. Brandt, H. Kostial, T. Hesjedal, M. Ramsteiner, and K. H. Ploog, "Crack-free and conductive Si-doped AlNGaN distributed Bragg reflectors grown on 6H-SiC(0001)," *Appl. Phys. Lett.*, vol. 85, 1970, Sept. 2004.

[9] J. K. Kim, Y.-H. Cho, J. S. Kwak, O.-H. Nam, J. W. Lee, Y. J. Park, T. I. Kim, J. W. Kim, and J. L. Lee, "The Effects of Au Overlayer on the Thermal Stability of Pt Ohmic Contact on P-Type GaN," *J. Korean Phys. Soc.*, vol. 39, no. 1, pp. 23, July 2001.

[10] G. A. Smolyakov, V. A. Smagley, W. Nakwaski, P. G. Eliseev, and M. Osinski, "Design of InGaN/GaN/AlGaN VCSELs using the effective frequency method," *Proc. SPIE*, vol. 3625, pp. 324–335, Jan. 1999.

[11] S.-R. Jeon, Y.-H. Song, H.-J. Jang, G. M. Yang, S. W. Hwang, and S. J. Son, "Lateral current spreading in GaN-based light-emitting diodes utilizing tunnel contact junctions," *Appl. Phys. Lett.*, vol. 78, 3265, May 2001.

[12] W. Nakwaski, M. Wasiak, P. Mackowiak, W. Bedyk, M. Osiñski, A. Passaseo, V. Tasco, M. T. Todaro, M. De Vittorio, R. Joray, J. X. Chen, R. P. Stanley, and A. Fiore, "Oxidation kinetics of AlAs and (AlGa)As layers in arsenide- based diode lasers: Comparative analysis of available experimental data," *Semicond. Sci. Technol.*, vol. 19, 333, March 2004.

[13] G. M. Yang, M. H. MacDougal, and P. D. Dapkus, "Ultralow threshold current ertical-cavity surface-emitting lasers obtained with selective oxidation," *Electron. Lett.*, vol. 31, no. 11, pp. 886–888, May 1995.

[14] J. Dorsaz, H.-J. Bühlmann, J.-F. Carlin, N. Grandjean, and M. Ilegems, "Selective oxidation of AlInN layers for current confinement in III–nitride devices," *Appl. Phys. Lett.*, vol. 87, 072102, Aug. 2005.

[15] M. Ferhata, J. Furthmuller, and F. Bechstedt, "Gap bowing and Stokes shift in $In_xGa_{1-x}N$ alloys: First-principles studies," *Appl. Phys. Lett.*, vol. 80, 1394, Feb. 2002.

[16] Gh. Alahyarizadeh, H. Aghajani, H. Mahmodi, R. Rahmani, and Z. Hassan, "Analytical and visual modeling of InGaN/GaN single quantum well laser based on rate equations," *Optics & Laser Technology*, vol. 44, no. 1, pp. 12–20, Feb. 2012.

[17] J. F. Carlin, J. Dorsaz, E. Feltin, R. Butté, N. Grandjean, M. Ilegems, and M. Laügt, "Crack-free fully epitaxial nitride microcavity using highly reflective AlInN/GaN Bragg mirrors," *Appl. Phys. Lett.*, vol. 86, 031107, Jan. 2005.

[18] D. K. Hwang, S. H. Kang, J. H. Lim, E. J. Yang, J. Y. Oh, J. H. Yang, and S. J. Parka, "p-ZnO/n-GaN heterostructure ZnO light-emitting diodes," *Appl. Phys. Lett.*, vol. 86, 222101, May 2005.

[19] G. Kipshidze, V. Kuryatkov, B. Borisov, M. Holtz, S. Nikishin, and H. Temkin, "AlGaInN-based ultraviolet light-emitting diodes grown on Si.111.," *Appl. Phys. Lett.*, vol. 80, 3682, May 2002.

1 Introduction

In these years, III-V nitride semiconductors are very attractive owing to their wide direct band gap, and Their ternary alloys are ideal for fabrication of optoelectronic devices such as light emitting diodes (LEDs), laser diodes (LD) and vertical cavity surface emitting lasers (VCSELs). The main advantages of the VCSELs are numerous such as circular output beam, single longitudinal mode operation and low beam divergence [1, 2, 3].

In the VCSEL, optical mode confinement is present in the center of the VCSEL and the essential problem is the focusing of the carrier density in this part of the device. Optically pumped nitride-based VCSELs have already been reported [4]. For electrically pumped VCSELs, the realization of high quality GaN-based distributed Bragg reflectors (DBRs) is necessary [5, 6]. N-type doping of nitride-based DBRs has already been demonstrated [7, 8], however injection of current laterally is still difficult due to the relatively low conductivity of p-type GaN [9]. Consequently in GaN-based VCSELs, to find a way for injection of current laterally and formation of a high-quality DBRs are very important. Nowadays, in a GaN-based VCSEL, in order to localize current injection under a mirror, an intra-cavity contact is used to spread the current laterally and then it is injected to the active region [10]. A tunnel junction (TJ) structure in GaN-based devices is presented in order to improve the lateral conductivity [11].

Selective oxidation is a widely used technique in the AlAs/GaAs system [12] for successful current confinement schemes in GaAs-based VCSELs [13]. Dorsaz *et al.* reported a procedure allowing for selective anodic oxidation of lattice-matched AlInN layers and its application to the fabrication of light-emitting diodes (LEDs) [18]. Using this technique, they have laterally oxidized buried AlInN layers over several tens of micrometers. In our study, we applied the AlInN oxided layer for lateral injection current confinement in the GaN-based VCSEL structure [14].

Although the oxide aperture size behavior in VCSEL has been investigated by several researchers, but to the authors' knowledge, little research has been done for GaN-based VCSEL in this area so far. This paper is a numerical study of the aperture diameter effect on the electrical properties of the GaN-based intracavity-contacted oxide-confined VCSEL and the influence of the oxide aperture on the VCSEL threshold current using Integrated System Engineering Technical Computer Aided Design (ISE TCAD).

2 VCSEL design

Advanced numerical simulation software with cylindrical symmetry was used in order to analyze the performance of GaN-based VCSELs. The drift diffusion transport equations and Poisson equation for electrons and holes are solved.

The bandgap energies of the $In_xGa_{1-x}N$ and $Al_xGa_{1-x}N$ ternary alloys at room temperature are given by [15]:

$$E_{g,In_xGa_{1-x}N} = xE_{g,InN} + (1-x)E_{g,GaN} - 1.43x(1-x) \qquad (1)$$

$$E_{g,Al_xGa_{1-x}N} = xE_{g,AlN} + (1-x)E_{g,GaN} - 1.3x(1-x). \qquad (2)$$

The Shockley Read-Hall (SRH) recombination lifetime of the carriers is assumed to be 1 ns. However, due to the sensitivity of the type and density of recombination centers to the technological process, it is a rough estimate. Table I shows the binary nitride materials parameters that have been used in our simulation [16].

Table I. Binary III- nitride materials parameters at room temperature [16]

Parameters	Symbol (unit)	GaN	InN	AlN
Dielectric constant	ε	9.5	15.3	8.5
Refractive index near E_g	n	2.5067	2.9	2.035
Band gap energy	E_g (eV)	3.425	0.77	6.28
Electron diffusion constant	D_n (cm^2/Vs)	39	80	7
Electron affinity	χ (eV)	4.1	5.7	1.9
Electron effective mass	m_e (m_0)	0.22	0.11	0.4
Heavy hole effective mass	m_{hh} (m_0)	1.595	1.44	3.53
Light hole effective mass	m_{lh} (m_0)	0.26	0.157	0.26

For simulated structure design, we developed the structure in Ref. [14] and the Ref. [17] has been used also. In VCSEL the cavity included the cladding layers and active region that are sandwiched between two distributed Bragg reflectors. The active region in this device consists of the $In_xGa_{1-x}N$ layers with 0.13 indium composition for wells and 0.01 indium composition in InGaN barrier layers. This region has been sandwiched between two p-type and n-type cladding layers of $Al_xGa_{1-x}N$ with 0.1 mole fraction. The active medium for the double quantum well consists of two quantum wells and three barriers. In this GaN-VCSEL, DBRs includes GaN and $Al_xIn_{1-x}N$ layers with 0.82 indium mole fraction. DBRs consist of 23 pairs of p-type doped layers at the top and 28 pairs of n-type DBRs at the bottom. One $Al_{0.62}InN$ selective oxidation layer with aperture diameter of 5 μm has been used for the current confinement [14]. The doping concentration of the p and n-type layers is 1.4×10^{18} cm^{-3} and 8×10^{17} cm^{-3} respectively. Hole and electron mobilities are 8 and 200 cm^2/Vs, respectively [18, 19]. The mesa diameter is 7 μm and the emission wavelength of VCSEL is about 414 nm.

3   Results and discussion

The simulated GaN-based VCSEL structure is illustrated in Figure 1 (a). Figure 1 (b) shows the I–V characteristics of an oxidized GaN-based VCSEL. This diagram shows the insulating behavior of the oxide AlInN layer on the electrical characteristics of the VCSEL. From this figure it is observed that differential resistance of the VCSEL increases with the reduction of the current aperture diameter that is in agreement with the experimental result [14]. This is due to the cross-sectional area reduction of the oxide aper-

ture. The reliability and thermal property of the VCSEL will be destroyed by the increasing resistance. Consequently the low differential resistance in the VCSEL is important.

In Figures 1 (c), the electrostatic potential versus the vertical position with oxide aperture diameter changing are illustrated. From this figure, it is observed that with oxide aperture diameter increasing, the electrostatic potential decreased. As already mentioned, differential resistance of the VCSEL reduced with the current aperture diameter increasing. Consequently electrostatic potential decreased and to achieve lasing operation, higher injection current is necessary.
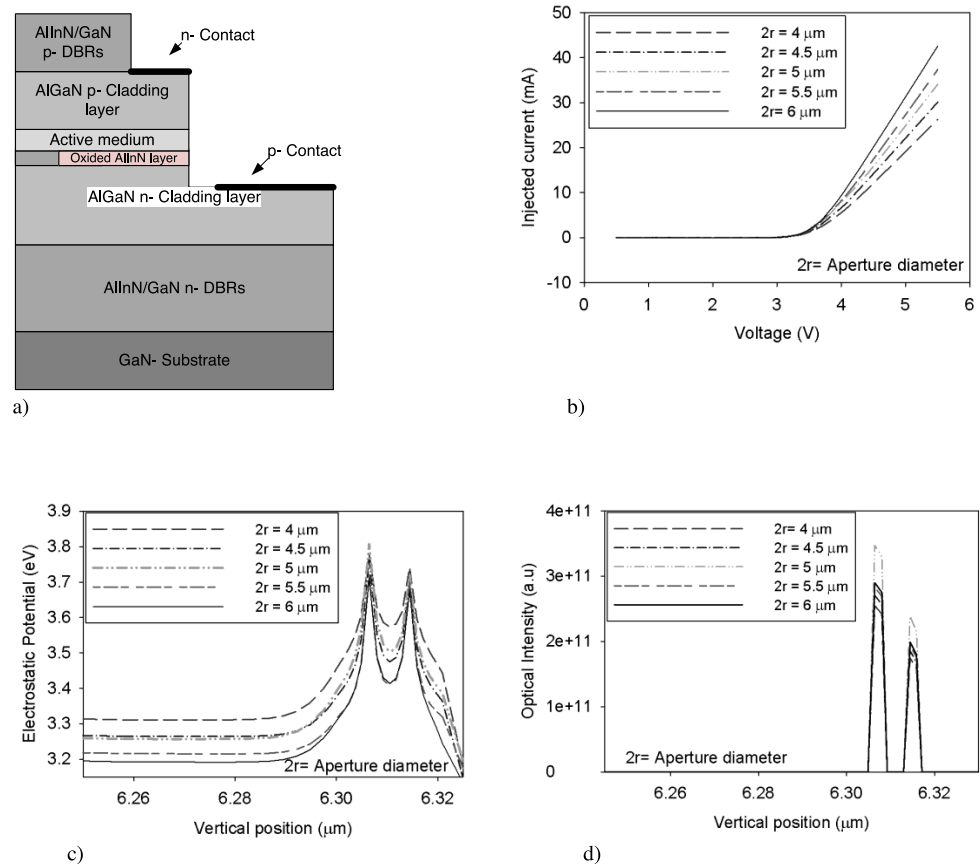

Fig. 1. a) Schematic illustration of GaN- based multi quantum wells VCSEL, b) voltage as a function of injected current, c) electrostatic potential as a function of vertical position and d) optical intensity versus the vertical position for GaN-based VCSEL structure with oxide aperture diameter (2r) changing from 4 to 6 μm at 300 K.

The influence of the oxide aperture diameter on the threshold current and output power of the GaN-based VCSEL is investigated. The simulation results at 300 K are listed in Table I. When the aperture diameter increases from 4 μm to 6 μm by step of 0.5 μm, the threshold current increases from 12.127 mA to 22.659 mA. It is due to the increasing electron-hole wave func-

tion separation that leads to the lateral leakage enhancement which is important for the threshold current. In VCSELs with smaller aperture sizes, lateral confinement of carriers and optical field is better. In VCSELs with larger aperture sizes, the higher injection current is necessary to achieve lasing operation.

Table II. Threshold current, output power and optical confinement factor versus the aperture diameter in the GaN-based VCSEL at 300 K

Aperture diameter (μ m)	Threshold current (mA)	Output power (mW)	OCF
4	12.127	8.795	0.00744909
4.5	12.753	9.775	0.00744910
5	13.523	12.290	0.00749172
5.5	16.166	10.562	0.00744914
6	22.659	10.814	0.00744917

We observed that with oxide aperture diameter increasing from 4 to 5 μm by step of 0.5 μm, the output power increased from 8.795 to 9.775 mW. This is attributed to increasing radiative recombinations inside the active region due to more confined lasing modes inside the active medium. The decrease in output power from decreasing of oxide aperture diameter from 5 to 6 μm by step of 0.5 μm is attributed to the saturation of the active region by carriers. Some of carriers could escape from the MQWs active region which caused the decrease in the output power. In 5 μm oxide aperture diameter, the output power reaches the maximum value of 12.290 mW which is the optimal value for the output power. It is related to the highest optical confinement factor (OCF) for 5 μm aperture diameter. VCSEL has the highest optical intensity for this diameter as illustrated in Figure 1 (d). For this diameter, there is a balance between the threshold current and output power.

4   Conclusion

We have investigated the effect of aperture diameter in intracavity-contacted oxide-confined GaN-based vertical cavity surface emitting lasers. The electrical characterization of the oxidized device shows an enhancement in the differential resistance of the VCSEL with the reduction in the current aperture diameter. An enhancement in the VCSEL threshold current was observed with the oxide aperture diameter increasing. Maximum output power and high optical intensity were observed when the diameter of the oxide aperture was 5 μm. In this case, the optical confinement factor has the highest value.

Acknowledgment